



Eco-Friendly Silver Nano Films for the Adsorption of Fluoride Ions Based on Light Scattering Phenomenon

V. Durga Praveena¹, K. Vijaya Kumar^{2*}

¹Department of Chemistry, SASJ GDC, Narayanapuram-534406, A.P, India.

²Department of Physics, KL University, Guntur-522502 State, A.P, India.

Abstract : Nano silver particles embedded with chitosan have been synthesised by non-toxic green method and characterised by UV-VIS, FTIR, FESEM, EDS and XRD. The formation of silver nanoparticles is characterised by UV-VIS Spectroscopy which shows a characteristic absorption band at 454 nm. The Field Emission Scanning Electron Microscope (FESEM) images confirm the presence of Ag NPs. The crystal structure and the average particle size of 20nm was estimated by using XRD. The film has been shown to be effective for the detection and the removal of one of the inorganic pollutant fluorides from natural wastes and wastewaters within the response time of 2-3 sec. This novel technique provides a selective methodology for the removal of fluoride ions and has been satisfactorily applied to its quantification in parenteral solutions.

Keywords: Silver nano particles, FESEM, XRD, UV-VIS, FT-IR, fluoride ions.

1. Introduction:

The quality of water was analysed on the basis of colour, odour, and taste. People exploit water from ponds, lakes and rivers for drinking. Owing to the augment in population and pollution of the environment, the quantity of surface water¹ i.e., available dwindle with time and most of it capitulate to severe pollution. Different contaminants are released to water bodies due to the rapid industrialization of human society, including heavy metal ions, organics, bacteria, viruses, and so on, which are serious harmful to human health^{2,3} (Wang et al. 2012).

Fluoride is a health affecting substance which is not a nutrient. The concentrations of F- IN ground water vary significantly from place to place. The presence of fluoride naturally occurs through rock and soil formation in the form of flourspar, fluorapatite, geochemical deposits, amphiboles, natural water systems and earth crust⁴. In addition to this fluoride can also be found in various Industrial work, chiefly electroplating, semiconductor, glass, ceramic and fertilizer industries⁵.

Fluoride enters the body through drinking water as a major source of daily intake. According To WHO The acceptable fluoride concentration in drinking water is in the range of 0.5 to 1.5 mg/l⁶. F⁻ effects the metabolism of elements such as Ca, P in human body and lead to dental and skeletal fluorosis due to its high electro negativity^{7,8}. Plants and animals also adversely affected by Excess fluoride. Needle scratch, tip burn diseases and inhibition on plant metabolism leading to necrosis were the effects of excess F⁻ on agriculture. The prominent symptoms of fluorosis were also observed in the animals.

Because of these reasons the pollution of ground water by fluoride contamination has been a major concern⁹. The problems in connection with fluoride ion pollution could be reduced or minimized by precipitation¹⁰, ultrafiltration, electrode-deposition, reverse osmosis, etc., but these processes have flaws such as high cost, low removal efficiency and generation of secondary pollutants.

Nanotechnology plays an important role for the sensing and removal of pollutants. Nano materials has been found to be an effective and economic with high potential for the purification of water¹¹. Due to their unusual reactivity, surface-volume ratio as well as size dependent physical, optical and chemical properties¹². Many nano systems such as nano scale grapheme¹³, grapheme oxide, metal oxide composites, carbon nanotubes, zerovalent iron^{14,15}, Al, Ti, Mg, Ce, Mn, Zn, noble metals (Ag, Au, Cu) for the treatment of water¹⁶⁻¹⁹. Application of Noble metals, even though not in nano form, they were damaging the DNA of bacteria. Nano zero valent silver, a recently discovered technology, is being used to successfully treatment various heavy metal ions in aqueous solutions²⁰⁻²².

AgNps have also been widely used in sensing applications for a variety of inorganic pollutants. In the present study we employed a spectrophotometric method for the detection and deduction of fluoride ions using nano silver coated chitosan biofilm (AgNps/CS).

2. Experimental:

2.1 Materials

Chitosan (degree of deacetylation: 79%, molecular mass: 500,000 g/mol) was purchased from sea foods (Cochin), India. AgNO₃ was purchased from Aldrich and used without further purification. The other chemicals were analytical grade from Fischer Scientific without further treatment. All aqueous solutions were made using ultrahigh purity water purified using a Mill-Q Plus system (resistivity = 18 M Ω cm) (Millipore Co.).

2.2 Preparation of plant extract

The fresh leaves of *Achyranthes aspera* were collected from the surrounding areas of W.G.Dt and were washed several times with millipore water to remove dust then it was cut into small pieces. 5 g of thoroughly washed leaves were heated in 250 ml of millipore water for 15 min in an Erlenmeyer flask using a water bath then the solution is filtered using what man no.4 filter paper. The filtered leaf extract was stored in a cooled atmosphere for further use^{23,24}.

2.3 Preparation of silver nano particles

The Silver nitrate solution was reduced using plant extract at room temperature, resulting in a light yellow colour solution indicating the formation silver nano particles²¹.

2.4 Characterization of synthesized silver nanoparticles

The characterisation of AgNp/CS thin film has been evaluated by FESEM, EDS, FTIR, UV-VIS and XRD. Field Emission Scanning Electron Microscope (Nova Nano FE-SEM 450 Model) was used to obtain SEM images at an accelerating voltage of 200 kV. The presence of Ag has been confirmed by EDS spectrum. Absorption spectra of the samples were taken on a UV-VIS double beam spectrophotometer (JASCO model V-670) with a range of 300-580 nm. X-Ray Diffractometer (PAN Analytical X'Pert Pro) was used to analyze the crystallographic studies of Ag-CS thin film. FTIR spectra were recorded in a Perkin Elmer Version 10.03.06.

2.5 Deposition of Silver Nanoparticles in Chitosan matrix

The CS was prepared by the method described below: 2 g CS was dissolved in 200 ml 2% (V/V) acetic acid solution under magnetic stirring. When the solution became clear, Silver nanoparticles, Chitosan solutions were mixed in 2:3 ratio. Finally, films were made by casting the solution on the glass slides, dried at room temperature. A range of AgNP/CS concentrations were used to treat the bacteria and for other experiments in this study.

2.6 Sensing study of Fluoride ions

For the sensing study 1×10^{-3} M of Sodium fluoride solution is used. Fluoride concentration is varied by diluting fluoride solutions of different concentrations (1 to 100 ppm in deionised distilled water) were prepared right before experiment.

3 Results and discussions

3.1 FTIR spectra of Chitosan and its derivative

FTIR spectra were recorded in a Perkin Elmer version 10.03.06, Spectrophotometer. The spectral band for chitosan appear at $3,526 \text{ cm}^{-1}$ (axial OH group), $3,337 \text{ cm}^{-1}$ (N-H stretching), $2,364 \text{ cm}^{-1}$ (CN asymmetric band stretching), $1,754 \text{ cm}^{-1}$ (amide linkage), $1,673 \text{ cm}^{-1}$ (CO band stretching), $1,523 \text{ cm}^{-1}$ (NH angular deformation in CONH plane), $1,320 \text{ cm}^{-1}$ (CN band stretching, axial deformation of amino group) and $1,140$ - $1,026 \text{ cm}^{-1}$ (ether linkage, C-O-C band stretching).

In AgNp/CS, (Fig.1) shows bands are shifted to higher frequencies i.e, 3353.51 cm^{-1} (overlap of O-H and N-H stretching vibrations), 2922.34 cm^{-1} (C-H stretching), 1744.89 cm^{-1} , 1728.74 cm^{-1} (NH₂ bending, amide linkage), 1569.07 cm^{-1} , 1411.41 cm^{-1} , 1070.14 cm^{-1} , 649.17 cm^{-1} [C-C, C-O (esters and ethers) and C-O (polyols)] more pronounced shift in the FTIR spectrum could be observed in the complexes (Fig. 1(b) inside). The major differences are: the peak at $3,526 \text{ cm}^{-1}$ corresponding to the stretching vibration of amino group (-NH₂) and hydroxyl group (-OH), shifted to lower frequency (3339 cm^{-1}), and the peak of 3339 cm^{-1} becomes wider, which indicates hydrogen bonding is enhanced and may be explained as that the additive effect of water absorbed on the surface of Ag nanoparticles and the -OH group of CS. This suggests that NPs were capped by the polymer.

The polar groups O-H of polysaccharide have the good ability of coordination reaction with metal ions (e.g., with silver ions). When O-H groups and silver ions form coordination bonds, the interactions among the resultant Ag particles and oxygen atoms of O-H groups become stronger with increasing amount of Ag. This can lead to corresponding changes both in the positions and in the strengths of IR spectra of CS.

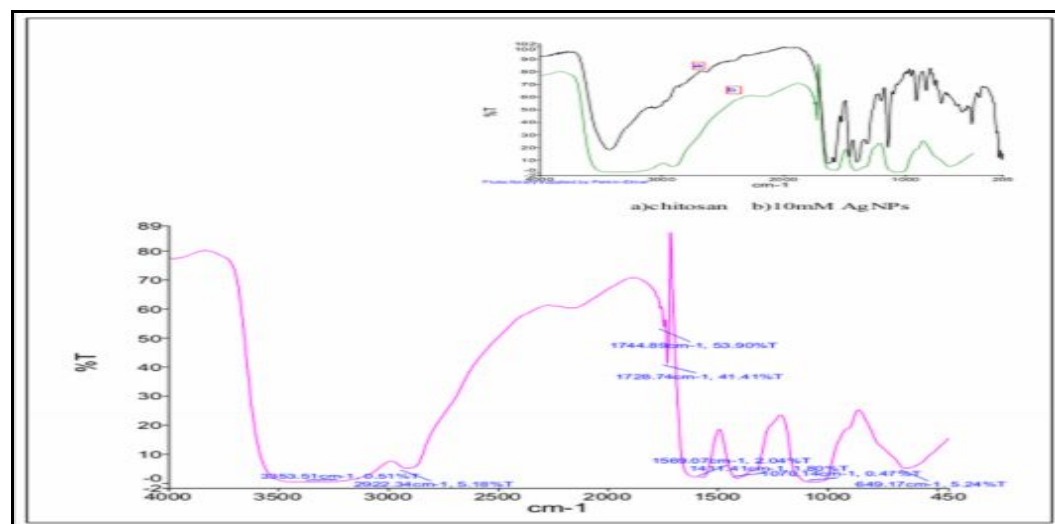


Figure 1. FT-IR Spectra of AgNps/CS film

3.2 XRD

The XRD pattern was recorded by X-ray diffractometer (PAN Analytical X' Pert, Almelo, The Netherlands) equipped with Ni filter and $\text{CuK}\alpha$ ($\lambda = 1.54056 \text{ \AA}$) radiation source.

Fig 2 shows the XRD pattern for silver nanoparticles synthesized using natural plants extract and the diffraction peaks were found to be broad around their bases indicating that the silver particles are in nanosizes.

The mean particle diameter of silver nanoparticles was calculated from the XRD pattern according to the line width of the plane, reflection peak using the following Scherrer's equation (Balaji et al., 2009)²⁵: The equation uses the reference peak width at angle θ , where k is the X-ray wavelength (1.5418 Å), $\beta^{1/2}$ is the width of the XRD peak at half height and K is a shape factor. The particle sizes of the samples in our study have been estimated by using the above Scherrer's equation²⁰ and was found to be ~17nm for the strongest peak.

$$D = \frac{K \lambda}{\beta^{1/2} \cos \theta}$$

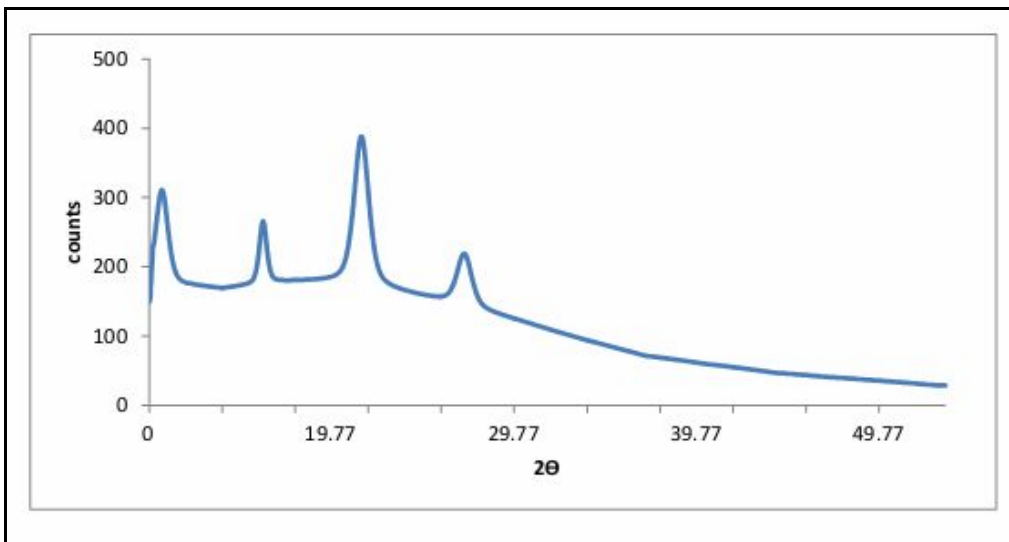
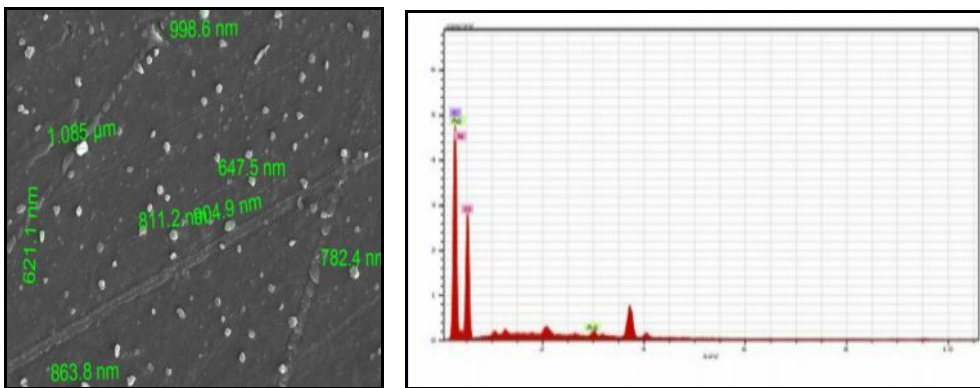


Figure 2. XRD Spectra of AgNPs/CS film



(a)

(b)

Figure 3 (a) SEM image of the AgNPs/CS using *Achyranthesaspera.L*, extracts (b) EDS Spectra of Silver nanoparticles.

3.3 UV-VIS Spectroscopy

UV-visible spectroscopic data of Each sample was analyzed by UV-visible spectrophotometer (Jasco V-670) in the range 250-750 nm and the wavelength corresponding to maximum absorption (λ_{max}) was recorded which are identical to the characteristics UV-visible spectrum of metallic silver nanoparticles. Chitosan in 1% (v/v) acetic acid is used as blank.

Silver nanoparticles absorb radiation in the visible region of the electromagnetic spectrum (380–450 nm) due to the excitation of Surface plasmon vibrations, and this is responsible for the striking yellow–brown color of silver nanoparticles.

Silver nanoparticles stability was checked up to six months and it was found that stability is nearly constant even up to six months. Due to VanderWaals forces or Coulomb's forces of attraction the individual particles have a tendency to form large sized agglomerates during the preparation of silver nanoparticle suspension. Chitosan is used as a stabilizer in order to prevent the agglomeration of small particles which can form a protective layer on the particle's surface. A strong physical adsorption of the CS onto the surface of the silver nanoparticles is also an indication of better stabilization. The evolution of UV-vis absorption spectrum of silver nanoparticles embedded in chitosan film we prepared is shown in Fig. 4b. A plasmon absorbance of the film was observed between 410–450 nm.

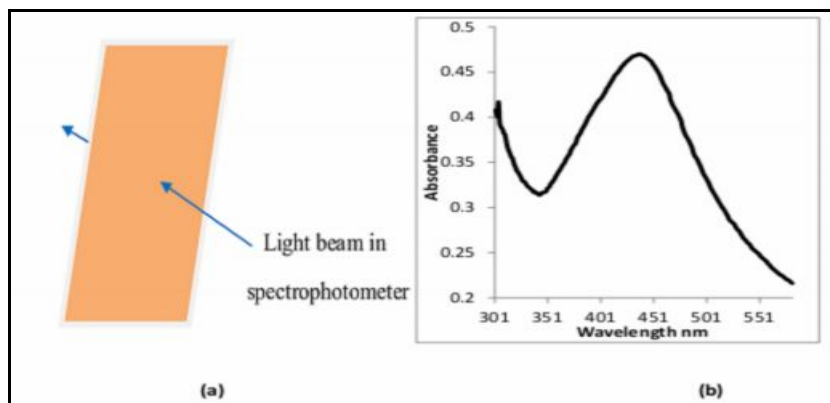


Figure 4. (a) Schematic diagram of the AgNps/CS thin film sensor; path of the light beam in the spectrometer is shown. (b) Surface plasmon resonance (SPR) spectrum, of the AgNps/CS.

3.3.1. Effect of reaction duration

The formation of silver nanoparticles was evidenced with the change in colour of the solution from colourless to light yellowish colour. The formation of silver nanoparticles was monitored through UV-VIS spectrophotometer at different time intervals (Fig. 5). The spectrum obtained at 90 min shows the absorption maximum at 454nm. The intensity of the peak with respect to the height increases gradually with increase of time. There was no change in peak position for 10 hrs to 24hrs. Now these nanoparticles can be embedded in chitosan for further application.

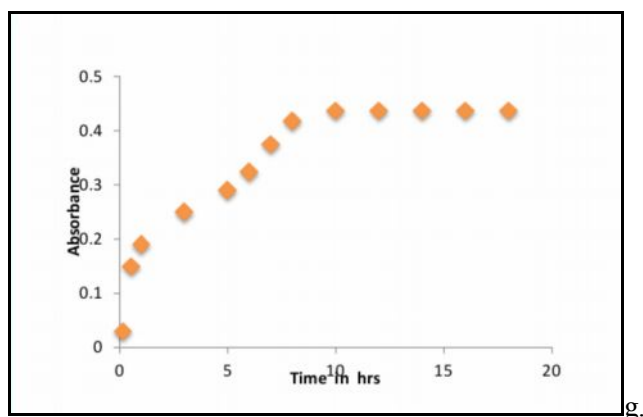


Figure 5. Changes in the SPR band of the AgNps at various time intervals using UV-vis spectrophotometer.

3.4 Dissolution and swelling test of chitosan based silver nano particles

The swelling studies of chitosan based silver nano particles were carried out in distilled water at room temperature for a period of 24 hrs the percentage of swelling of these films were calculated by using the eq.1:

$$\text{Percentage of swelling} = \frac{WS - W}{W} \times 100\%$$

Where, W_s is the weight of swollen chitosan film (g) and W is the weight of dry chitosan film.

It was observed that chitosan film had 37.5% swelling when allowed to remain in distilled water for 24hrs at room temperature.

Sensing Experiments.

All experiments (except those related to the temperature dependence) were carried out at the ambient temperature of 25°C. The sensor film (Figure 4a) was immersed in ultra pure water (Millipore Milli-Q, resistivity = 18 M Ω cm) then placed in a spectrometer; the SPR spectrum of the film was monitored at first time. The water was removed and replaced with the analyte solution. The SPR spectrum of the film was recorded. A fresh film was used for each new experiment. The reproducibility of the sensing process was examined by running repeated batches of selected experiments.

3.4 Fluoride sensing of green AgNPs/CS film

To investigate the sensitivity effect of the AgNP toward F^- ion, Fluoride ions with the concentrations of 2 to 25 mg/L was added to the AgNP/CS film. The sensing ability and selectivity of the prepared AgNps were studied by using UV/VIS spectroscopy. On interaction of F^- ions with AgNps, F^- undergoes diffusion into the polymer matrix during which the metal changes into metal salt. A clear blue shift of the peak is observed at higher concentrations of F^- . This aspect can be exploited by including the peak shift, $\Delta A = [A_{\max}(0) - A_{\max}(t)]$ in the sensor response. This is due to the fact that, degradation of F^- takes place with the formation of AgNP- F^- surface complex.

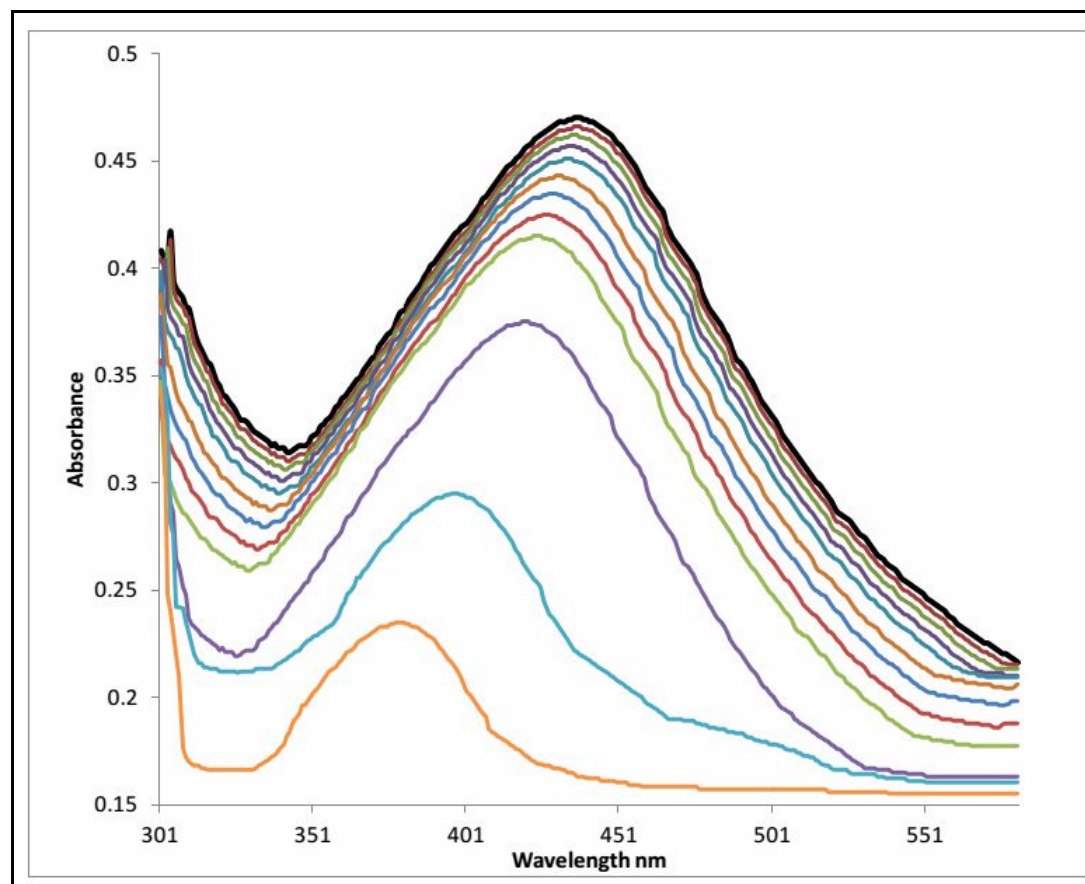


Figure 7. UV-vis absorption response of green AgNP-CS film upon addition of different concentration of F^- ions.

The absorbance spectra for a set of selected concentrations are shown in Figure 7; For each measurement, fresh film of AgNPs/CS are taken. The spectra show small but definite and reproducible decrease in intensity within a few minutes. In addition to the decrease in intensity, the peak undergoes a blue shift which becomes prominent at higher concentrations and the LSPR peak intensity at 437 nm decreases and another peak appears at 379 nm as the F^- content is increased. Change in absorbance at two different wavelength as a function of F^- concentration are provided in Fig.8(a). We have plotted absorbance ratio(Abs 379/Abs437) as a function of F^- concentration in Fig. 8(b). Within the range of 2 to 25 mg/L the absorbance ratio is almost linear, which indicates that the AgNPs/CS film is active for detection and removal of F^- content in the solution.

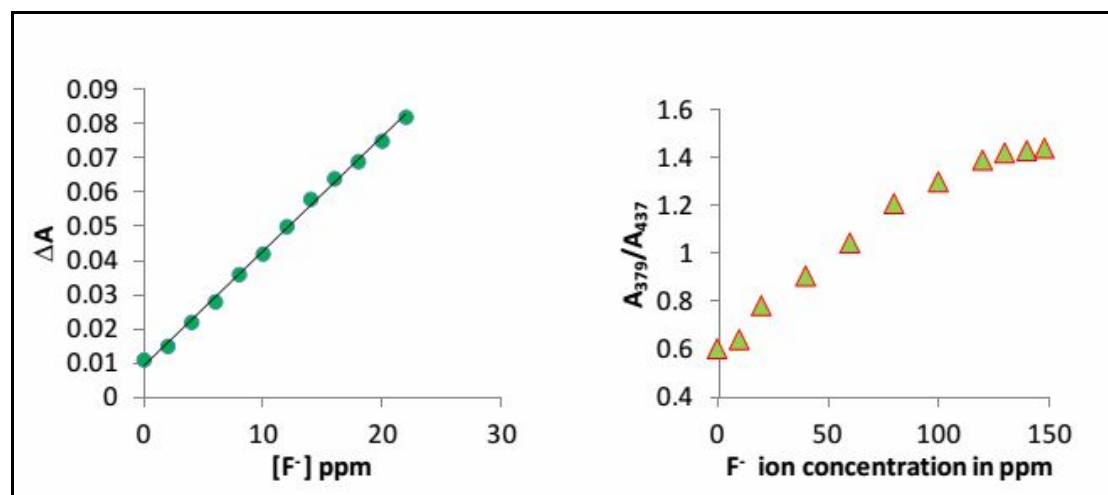


Figure 8. (a) Plot of absorbance intensity at 379 nm versus F^- concentration. (b) Ratio of the absorbance peak (Abs₃₇₉/Abs₄₃₇) for a silver nanoparticles solution exposed to increasing F^- content .

4. Conclusion

The silver NPs dispersion in a chitosan bio polymer matrix played a more important role in colorimetric sensing applications. In this study we have shown the feasibility of forming silver nanoparticles from silver nitrate through green process using aqueous extract of *Achyranthes aspera*.L,. Based on the unique LSPR properties of metallic nanoparticles, Colorimetric assays have showed to be very useful due to their simplicity, high sensitivity, low detection limit, low cost, fast response time and great reproducibility. The present study reports the application of nanoparticles for the removal of nitrite ions using AgNPs-CS film with high selectivity and sensitivity over Mn^{+2} , Fe^{+3} , CO^{+2} , Ni^{+2} , Zn^{+2} , K^+ , Mg^{+2} , Ba^{+2} ions. Keeping these significance properties in mind, in the near future we can use this thin film as a filter to remove inorganic pollutants for the water purification at room temperature .

Supplementary Information

All additional information pertaining to characterization of the complexes using FT-IR spectra (figure S1), XRD, SEM (figures S2,S3), UV-VIS (figures S4,S5,S6) and absorption response curves.SEM images by the introduction of nitrite ions (figures S7,S8,S9) are given in the supporting information available at www.ias.ac.in/chemsci.

Acknowledgements

The authors express their gratitude to the Center for NanoScience and Technology KL University, For the support of this work. We also thank the Materials Research Center, Malaviya National Institute of Technology, Jaipur, for providing the FESEM-EDS and XRD data.

References:

1. Hazen Drive ,2009 *Environmental services Concord* New Hampshire 03301(603)271-3503.
2. WHO 1985a Guidelines for the study of dietary intake of chemical contaminants. Geneva, *World Health Organization Offset Publication No. 87*.
3. United States Environmental Protection Agency, National Primary Drinking Water Regulations: Contaminant Specific Fact Sheets, Inorganic Chemicals, Consumer Version. Washington, DC, 1995.
4. Toyoda A, Taira A . A new method for treating fluorine wastewater to reduce sludge and running costs .IEEE Trans, Semiconductor Manufacture., 2000, 13: 305-309.
5. WHO and UNICEF 2010 Progress on Sanitation and Drinking-Water., Geneva, Switzerland.
6. Zhu CS, Bai GL, Liu XL, Li Y. Screening high-fluoride and high-arsenic drinking waters and surveying endemic fluorosis and arsenic in Shaanxi province in western China. *Water Research.*, 2006, 40: 3015-3022.
7. Bishnoi M, Arora S. Potable groundwater quality in some villages of Haryana, India: Focus on fluoride *J Environ Biol.*, 2007, 28: 291-294.
8. Shailaja K, Johnson MEC . Fluorides in groundwater and its impact on health. *J Environ Biol.*, 2007, 28: 331-332.
9. Tripathy SS, Bersillon JL, Gopal K. Removal of fluoride from drinking water by adsorption onto alum-impregnated activated alumina. *Sep Purif Technol.*, 2006, 50: 310-317.
10. Auffan M, Rose J, Bottero J.Y et al., Towards a definition of inorganic nanoparticles from an environmental, health and safety perspective. *Nat. Nanotechnol.*,2009, 4: 634 -641.
11. Pradeep T and Anshup. Noble metal nanoparticles for water purification: A critical review. *Thin Solid Films.*, 2009, 517: 6441-6478.
12. Zhang, L.; Yi, M. Electrochemical nitrite biosensor based on the immobilization of hemoglobin on an electrode modified by multiwall carbon nanotubes and positively charged gold nanoparticle. *Bioprocess Biosyst. Eng.*, 2009 , 32 :485 – 492.
13. Uzum C, Shahwan T, Eroglu AE, Hallam KR, Scott TB, et al. Synthesis and characterization of kaolinite-supported zero-valent iron nanoparticles and their application for the removal of aqueous Cu²⁺ and Co²⁺ ions. *Appl Clay Sci.*, 2009, 43: 172-181.
14. Fakhri A, Adami S. Response Surface Methodology for Adsorption of Fluoride Ion Using Nanoparticle of Zero Valent Iron from Aqueous Solution. *J Chem Eng Process Technol.*, 2013, 4: 161-167.
15. Yuan, H.; Ma, W.; Chen, C.; Zhao, J.; Liu, J.; Zhu, H.; Gao, X. Shape and SPR evolution of thorny gold nanoparticles promoted by silver ions. *Chem. Mater.*, 2007, 19 :1592 – 1600.
16. Xiao, N.; Yu, C. Rapid-response and highly sensitive non-crosslinking colorimetric nitrite sensor using 4-aminothiophenol modified gold nanorods. *Anal. Chem.*, 2010 , 82 , 3659 – 3663.
17. Daniel, W. L.; Han, M. S.; Lee, J. S.; Mirkin, C. A. Colorimetric nitrite and nitrate detection with gold nanoparticle probes and kinetic end points. *J. Am. Chem. Soc.*, 2009 , 131 : 6362 – 6363.
18. A. J. Haes, R. P. Van Duyne. A nanoscale optical biosensor: sensitivity and selectivity of an approach based on the localized surface plasmon resonance of triangular silver nanoparticles. *J. Am. Chem. Soc.*, 2002, 124: 10596–10604.
19. Dubas ST, Pimpan V, Green Synthesis of Silver nanoparticles for Ammonia Sensing, *TALANTA.*,2008, 76 : 29-33.
20. G. V. Ramesh and T. P. Radhakrishnan , A Universal Sensor for Mercury (Hg, HgI, HgII) Based on Silver Nanoparticle-Embedded Polymer Thin Film *ACS Appl. Mater. Interfaces.*, 2011, 3: 988 – 994.
21. S. Pandey , Gopal K. Goswami, Karuna K. Nanda Green synthesis of biopolymer–silver nanoparticle nanocomposite: An optical sensor for ammonia detection *International Journal of Biological Macromolecules.*, 2012, 51 :583– 589.
22. V. Durga praveena and K. Vijay kumar . Physicochemical Studies On Nano Silver Particles Prepared By Green And Chemical Methods, *Advanced Materials Research.*, 2014, 938 :242-250.
23. V. Durga praveena and K. Vijay kumar , Green synthesis of Silver Nanoparticles from Achyranthes Aspera Plant Extract in Chitosan Matrix and Evaluation of their Antimicrobial Activities , *Indian Journal of Advances in Chemical Science.*,2014, 2 (3) : 171-17.
24. The XRD patterns were indexed with reference to the crystal structures from the ASTM chart card No.04-0783.
